A PMU-Based State Estimator for Networks Containing FACTS Devices

Wei Li
KTH Royal Institute of Technology
Stockholm, Sweden
wei3@kth.se

Luigi Vanfretti
KTH Royal Institute of Technology, Stockholm, Sweden
luigiv@kth.se
Statnett SF, Oslo, Norway
luigi.vanfretti@statnett.no

***Abstract*—This paper presents a PMU-based state estimation algorithm that considers the presence of flexible AC transmission system (FACTS). The models of FACTS devices, including thyristor- and converter-based devices, are developed and then combined with an AC network model. Considering the characteristics of PMU measurements, the network model for state estimation is separated from the measurements. By applying the nonlinear weighted least squares (WLS) algorithm, a PMU-based state estimator can estimate the states of an AC system and its embedded FACTS devices simultaneously. To validate the algorithm, simulation studies for a 9-bus system are performed.**

***Index Terms*—State estimation, Flexible AC transmission system, Phasor measurement units**

I. Introduction

A. Motivation

The flexible AC transmission system (FACTS) concept was introduced in the 90s and soon was recognized as a beneficial technology to enhance controllability and to increase power transfer capability [1] [2]. FACTS have become an indispensable asset to improve transmission quality and efficiency of existing AC grids. Therefore, FACTS devices have to be properly modeled and studied for power system operation and control.

One important and fundamental function of power system operation is state estimation (SE). SE is a process used to determine the state of a network by using measurements and a model of the grid. With a proper redundancy level, it can eliminate the effect of bad data and produce reliable state estimates in order to help operators monitor the grid and to support other analysis functions in an energy management system (EMS) [3].

Conventional SE uses measurements provided by supervisory control and data acquisition (SCADA) system with a rate of two to ten seconds per snapshot. This rate limits the speed at which SE can be executed. In this case, power system operation might benefit from a fast state estimator which can trace the dynamic behavior of power electronic devices, such as FACTS devices.

Wei Li is involved in the SweGRIDS program sponsored by the *Swedish Energy Agency*, *Svenska Kraftnät*, and *ABB*. Luigi Vanfretti is supported by *Statnett SF*, *STRONgrid*, and the *STandUP for Energy* collaboration initiative.

B. Previous work

In recent years, phasor measurement units (PMUs) have been widely implemented to complement conventional metering devices. PMUs provide GPS time-synchronized measurements at a rate of 30-50 samples per second. Hence, a PMU-based state estimator [4]- [7] could follow the trajectory of the power system and should sanitize data quickly to support other applications.

In addition, a conventional SE normally applies bus voltage magnitudes and angles as power system state variables, and bus voltage magnitudes, active power flows and injections, reactive power flows and injections as measurement variables. By its nature, the conventional network model and measurement model of the SE will contain numerous nonlinearities in contrast with circuit analysis models [8]. In contrast, a PMU-based state estimator applies voltage phasors at buses and current flow phasors on lines as both state variables and measurement variables, whose relations are based on the circuit analysis model. Therefore, a PMU-based SE deals with far less nonlinearities, leading to a much lighter computation burden.

C. Contributions

This paper proposes simplified FACTS devices' network models and corresponding measurement models to facilitate a PMU-based SE algorithm. This algorithm is then illustrated though simulation studies on a 9-bus system. The remainder of this paper is organized as follows. First, in Section II, a unified AC network branch model is presented for composing the entire AC network model. Second, Section III introduces the network models of different FACTS devices, including a static var compensator (SVC), a static synchronous compensator (STATCOM), a thyristor controlled series compensator (TCSC), and a static synchronous series compensator (SSSC). Then, Section IV briefly presents the proposed PMU-based SE algorithm together with its measurement model. Simulation results are shown in Section V, followed by conclusions in Section VI.

II. AC network branch model

PMUs measure voltage phasors $\tilde{\mathbf{V}}$ at the buses where PMUs installed and current phasors $\tilde{\mathbf{I}}$ on the lines adjacent to the

buses. Directly using $\tilde{\mathbf{V}}$ and $\tilde{\mathbf{I}}$ in the network model could significantly reduce the nonlinearity of network model and decrease the complexity of the associated Jacobian matrix. Based on these measured variables, a unified AC network branch model is proposed, which takes series impedance, shunt admittances, and transformers into account. Figure 1 shows its structure.

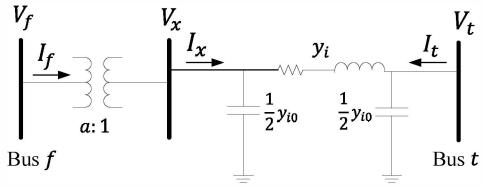

Fig. 1. AC line with transformer

The subscript $\boldsymbol{f}$ denotes the bus where current flows from and $\boldsymbol{t}$ is the bus where current flows to. An AC line can be represented by a line admittance y_i and a shunt admittance y_{io} in per unit. A transformer is represented by a tap ratio of $a : 1$. In the case of phase shifting transformers, a is a complex number. The model in Fig. 1 can be formulated as:

$$\begin{bmatrix} \widetilde{\mathbf{I_f}} \\ \widetilde{\mathbf{I_t}} \end{bmatrix} = \begin{bmatrix} \frac{\mathbf{y_i} + \frac{1}{2}\mathbf{y_{i0}}}{\mathbf{a}^2} & -\frac{\mathbf{y_i}}{\mathbf{a}^*} \\ -\frac{\mathbf{y_i}}{\mathbf{a}} & \mathbf{y_i} + \frac{1}{2}\mathbf{y_{i0}} \end{bmatrix} \begin{bmatrix} \widetilde{\mathbf{V_f}} \\ \widetilde{\mathbf{V_t}} \end{bmatrix}. \quad (1)$$

III. FACTS DEVICES' NETWORK MODEL

Depending on the types of power electronic components being used, FACTS devices can be classified as thyristor-based and converter-based devices. Thyristor devices have no gate turn-off capability while converter devices, i.e. voltage source converters (VSCs) and current source converters (CSCs), have gate turn-off capability. This characteristic results in differences, especially of control schemes, between these two types of FACTS devices. Thyristor-based FACTS include devices such as the SVC and TCSC; converter-based FACTS include devices such as the STATCOM and SSSC.

Note that both a thyristor-based and a converter-based devices with a similar control function will have a similar response within their linear operating range (under steady state conditions). Therefore, it is possible to categorize FACTS devices according to their functions. In this way, FACTS can be categorized as shunt devices, e.g., SVC and STATCOM, series devices, e.g., TCSC and SSSC, and combined series-series or series-shunt devices, e.g., UPFC.

This section will briefly present the network models of the SVC, STATCOM, TCSC and SSSC for the proposed PMU-based state estimation application. Other FACTS models can be easily obtained by modifying or extending these models with minor changes.

A. Shunt devices

A shunt FACTS device serves as a current source drawing from or injecting reactive current into the connected bus in order to effectively control the voltage at the bus. Voltage control is performed on the bus independently of the individual lines connected to it [1]. In addition, since shunt devices are not embedded in transmission lines, they do not need to sustain contingencies and dynamic overloads compared to series devices. However, shunt FACTS devices do not have the advantage of controlling power flow on lines and they are bigger than series devices for a required MVA size.

1) Static Var Compensator: An SVC is a variable shunt capacitor, which can be varied to maintain a constant voltage at the bus to which it is connected, as shown in Fig. 2(a). The firing angle (α) controls the turn-on period of the thyristor, hence varying the equivalent reactance of the SVC. To simplify the network model and reduce the number of state variables, the controlled variable is assumed to be an equivalent susceptance, b_{SVC}, as shown in Fig. 2(b).

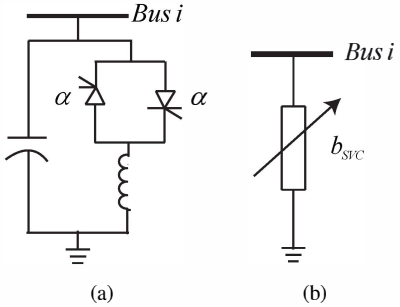

Fig. 2. SVC model schemes [1] [9]: (a) firing angle model; (b) equivalent susceptance model.

This network model can be formulated as:

$$\begin{cases} 0 = |\widetilde{V}_i| - V_i^{ref} \\ 0 = q_{svc} - b_{svc}|\widetilde{V}_i|^2 \\ Q_i^{ref} = |\widetilde{V}_i||\widetilde{I}_i|\sin(\theta_i - \delta_i) + q_{svc} \\ 0 = \widetilde{I}_i + \sum_{i=1}^{n} \widetilde{I_{ij}}, \end{cases} \quad (2)$$

where V_i^{ref} is the constant voltage which the SVC aims to maintain for Bus i; q_{svc} is the reactive power generated by the SVC and b_{svc} is the equivalent susceptance value; $\widetilde{V}_i$ and $\widetilde{I}_i$ represent the voltage phasor and the sum of injected line current phasors at Bus i; $\widetilde{I_{ij}}$ represents the current flow phasor in the direction of from Bus i to Bus j; and Q_i^{ref} is the reactive power reference for the load at Bus i, if Bus i has no load connected, Q^{ref} will be zero.

2) Static Synchronous Compensator: STATCOMs perform the same function as SVCs, i.e. to maintain the voltage at the connected bus. It can be VSC-based, as shown in Fig. 3(a), or CSC-based. Its model can be simplified as a current injection source for state estimation purposes, as shown in Fig. 3(b). The STATCOM current $\widetilde{I_{st}}$ is always in quadrature with the bus voltage $\widetilde{V}_i$, hence only reactive power is drawn or injected into the connected bus. Its network model can be formulated as:

$$\begin{cases} 0 = |\widetilde{V}_i| - V_i^{ref} \\ 0 = q_{st} - |\widetilde{V}_i||\widetilde{I_{st}}| \\ Q_i^{ref} = |\widetilde{V}_i||\widetilde{I}_i|\sin(\theta_i - \delta_i) + q_{st} \\ 0 = \widetilde{I}_i + \sum_{i=1}^{n} \widetilde{I_{ij}}, \end{cases} \quad (3)$$

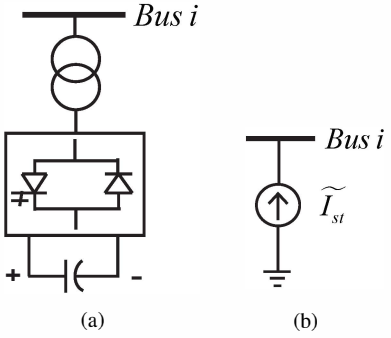

Fig. 3. STATCOM model schemes [1] [9]: (a) VSC-based STATCOM; (b) equivalent current source model.

where q_{st} and $\widetilde{I_{st}}$ are the reactive power and the equivalent current phasor generated by STATCOM, respectively; other notations are the same with those used in SVC model.

From Eq. (2) and (3), it can be observed that both SVCs and STATCOMs operate to maintain the bus voltage by manipulating the reactive power, but in different ways: SVCs are modeled as an equivalent susceptance b_{svc} while STATCOMs as a current source $\widetilde{I_{st}}$.

B. Series devices

A series FACTS device impacts the driving voltage and hence the current flow directly. Therefore, it allows to effectively control the current and power flows. Series FACTS devices have smaller size for the same MVA rating of a shunt device, but they have to be designed to be able to sustain different contingencies and overloads. This section presents two series FACTS devices, namely the TCSC and SSSC.

1) Thyristor Controlled Series Compensator: A TCSC allows varying the series reactance of a transmission line to regulate the active power flow through the line, as shown in Fig. 4(a). Although firing angle (α) is the control variable, an equivalent susceptance b_{tc} is used in order to simplify the network model and reduce the number of states variables, as shown in Fig. 4(b).

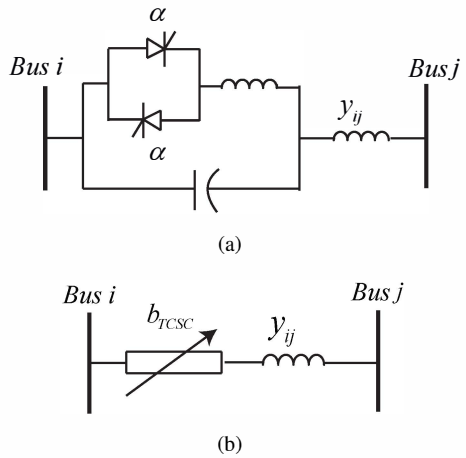

Fig. 4. TCSC model schemes [1] [9]: (a) firing angle model; (b) equivalent susceptance model.

This network model can be formulated as:

$$\begin{cases} 0 = P_{ij} - P_{ij}^{ref} \\ 0 = P_{ij} - |\widetilde{V_i}||\widetilde{V_j}|(y_{ij} + b_{tc})\sin(\theta_i - \theta_j), \end{cases} \tag{4}$$

where P_{ij}^{ref} is the constant active power flow reference on which the TCSC aims to maintain; y_{ij} is the line admittance without considering the TCSC and b_{tc} is the equivalent susceptance of the TCSC; θ_i and θ_j are the angles of voltage phasors $\widetilde{V_i}$ and $\widetilde{V_j}$, respectively.

2) Static Synchronous Series Compensator: An SSSC is a converter-based FACTS device as shown in Fig. 5(a). Its model can be simplified by a series voltage source for state estimation purposes, as shown in Fig. 5(b). An SSSC is able to provide a constant compensating voltage independently of variable line currents. This voltage V_{ss} is always in quadrature with the line current $\widetilde{I_{ij}}$, hence only its magnitude is controllable.

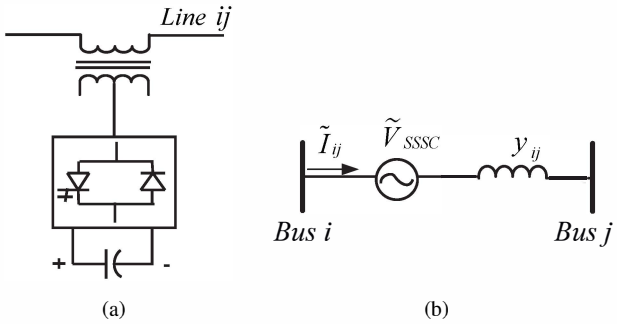

Fig. 5. SSSC model schemes [1] [9]: (a) VSC-based SSSC; (b) equivalent synchronous voltage source model.

In some cases, the injected voltage is assigned larger than the voltage difference between the sending- and receiving-end, that is, if $|\widetilde{V_{ss}}| > |\widetilde{V_i} - \widetilde{V_j}|$, the power flow will reverse. This bi-directional compensation capability distinguishes SSSCs from other series devices. However, in many practical applications, only capacitive series line compensation is required.

Generally, an SSSC has two control modes: in voltage compensation mode the SSSC can maintain the rated capacitive or inductive compensating voltage regardless of changing line current; in impedance compensation mode the SSSC is fixed to the maximum rated capacitive or inductive compensating reactance. Under constant voltage control mode, an SSSC can be formulated as:

$$\begin{cases} 0 = (\pm\widetilde{V_{ss}} + \widetilde{V_i} - \widetilde{V_j}) * y_{ij} - \widetilde{I_{ij}} \\ 0 = |\widetilde{V_{ss}}| - V_{ss}^{ref} \\ 0 = \theta_{ss} - \delta_{ij} - \pi/2, \end{cases} \tag{5}$$

where $\widetilde{V_{ss}}$ is the equivalent synchronous voltage of an SSSC and V_{ss}^{ref} is the constant voltage value on which the SSSC aims to maintain; θ_{ss} and δ_{ij} are the angles of SSSC equivalent voltage $\widetilde{V_{ss}}$ and line current $\widetilde{I_{ij}}$, respectively. Note that the $\pm$ symbol indicates the type of compensating voltage: a positive symbol indicates capacitive compensation and a negative symbol indicates inductive compensation.

Differently from (2)-(4) that are added into the system network model in addition to the AC network equations, Equation (5) replaces the corresponding (row) equations that are associated with the SSSCs in the AC network model, hence, the number of network equations remains the same. As phasors in the proposed state estimator are represented by magnitudes and angles, (5) is thus rewritten as follows:

$$\begin{cases} 0 = |\widetilde{V_{ss}}|y_{ij}cos(\delta_{ij}+\pi/2+\gamma_{ij}) + |\widetilde{V_i}|y_{ij}cos(\theta_i+\gamma_{ij}) \\ \quad -|\widetilde{V_j}|y_{ij}cos(\theta_j+\gamma_{ij}) - |\widetilde{I_{ij}}|cos(\delta_{ij}) \\ 0 = |\widetilde{V_{ss}}|y_{ij}sin(\delta_{ij}+\pi/2+\gamma_{ij}) + |\widetilde{V_i}|y_{ij}sin(\theta_i+\gamma_{ij}) \\ \quad -|\widetilde{V_j}|y_{ij}sin(\theta_j+\gamma_{ij}) - |\widetilde{I_{ij}}|sin(\delta_{ij}), \end{cases} \tag{6}$$

where θ_i and δ_{ij} are the angles of the voltage phasor and the line current phasor, respectively; γ_{ij} is the angle of the line admittance.

IV. Measurement model and the PMU-based State Estimation Algorithm

The conventional state estimation formulation for nonlinear systems is based on the nonlinear measurement model [3]:

$$\mathbf{z} = \mathbf{h}(\mathbf{x}) + \mathbf{e}, \tag{7}$$

where $\mathbf{z} \in \mathbb{R}^m$ is the measurement vector, $\mathbf{x} \in \mathbb{R}^n$ is the state vector, $\mathbf{h} : \mathbb{R}^n \to \mathbb{R}^m$ is a nonlinear function relating measurements to states, and $\mathbf{e} \in \mathbb{R}^m$ is the measurement error vector, which is assumed to have a normal distribution, i.e., $\mathbf{e} \sim \mathcal{N}(0, \mathbf{R_z})$. $\mathbf{R_z}$ denotes the corresponding measurement covariance matrix.

However, when PMUs are used for data acquisition, the state variables can be measured directly, i.e. $\widetilde{\mathbf{V}}$, $\widetilde{\mathbf{I}}$ phasors. A direct consequence is that the choice of state variables to be $\mathbf{z}$ in (7) can not be uniquely determined. Any variable chosen to be $\mathbf{z}$ in the measurement model will lose its corresponding element in the Jacobian matrix. In other words, the network model and corresponding Jacobian matrix lose their uniqueness. Based on above consideration, a new measurement model is needed to separate the measurement variables from the network model. The proposed measurement model is formulated as follows:

$$\mathbf{e} = \begin{bmatrix} \mathbf{h}(\mathbf{x}) \\ \mathbf{x} \end{bmatrix} - \begin{bmatrix} \mathbf{0} \\ \mathbf{z} \end{bmatrix} \tag{8}$$

where $\mathbf{h} : \mathbb{R}^n \to \mathbb{R}^k$, k is the number of network model equations. $\mathbf{h}(\mathbf{x})$ is the pure network model without measurements involved. The performance index $J(\mathbf{x})$ based on the proposed measurement model is expressed as follows:

$$J(\mathbf{x}) = \frac{1}{2}\left[\sum_{i=1}^{k}\left(\frac{h_i(\hat{\mathbf{x}})}{\sigma_i}\right)^2 + \sum_{j=1}^{m}\left(\frac{\hat{x_j} - z_j)}{\sigma_j}\right)^2\right], \tag{9}$$

where the inverse of σ_i^2 is the weighting of the i-th network equation in the WLS, the inverse of σ_j^2 is the weighting of j-th measurement. In order to minimize the estimation error, the performance index $J(\mathbf{x})$ should be minimized. This can be achieved when σ_i equals to the standard variance of the i-th network model equation error and σ_j equals to the standard variance of the j-th measurement.

Both Gauss-Netwon and Newton-Raphson methods can be used to solve the nonlinear WLS problem, which are described in the literature, e.g., [3].

Therefores, we directly apply the most commonly used iteration procedure to obtain the updated state $\hat{\mathbf{x}}$, as follows:

$$\begin{aligned} (\mathbf{H}^T(\hat{\mathbf{x}}^i)\mathbf{R}^{-1}\mathbf{H}(\hat{\mathbf{x}}^i))^{-1}\Delta\hat{\mathbf{x}}^i &= \mathbf{H}^T(\hat{\mathbf{x}}^i)\mathbf{R}^{-1}\Delta\mathbf{z}(\hat{\mathbf{x}}^i), \\ \hat{\mathbf{x}}^{i+1} &= \hat{\mathbf{x}}^i + \Delta\hat{\mathbf{x}}^i, \end{aligned} \tag{10}$$

where

$$\Delta\mathbf{z}(\hat{\mathbf{x}}^i) = \begin{bmatrix} \mathbf{h}(\hat{\mathbf{x}}^i)) \\ \hat{\mathbf{x}}^i - \mathbf{z} \end{bmatrix},$$

$\mathbf{H}(\mathbf{x})$ is the Jacobian matrix of the first order derivatives of $J(\mathbf{x})$, $\mathbf{R}$ denotes the covariance matrix with σ_i^2 and σ_j^2 on its diagonal.

V. Study cases

A 9-bus AC system, WSCC 3-generator 9-bus test system [10], was used to validate the proposed FACTS models and the SE algorithm. A one-line diagram of the test system is shown in Fig. 6. Synthetic measurements for off-line SE computations were obtained by running time-domain simulations in the Power System Analysis Toolbox (PSAT) [11], and 20 ms was selected as the step-size to mimic PMU data rate. For this test, all the weightings for network equations and measurements were assumed to be 1, and full measurement observability was assumed. With respect to different FACTS devices, they were placed in different positions according to their specific functions. Shunt devices were installed at bus 8, and series devices were installed on the line between bus 5 and bus 4.

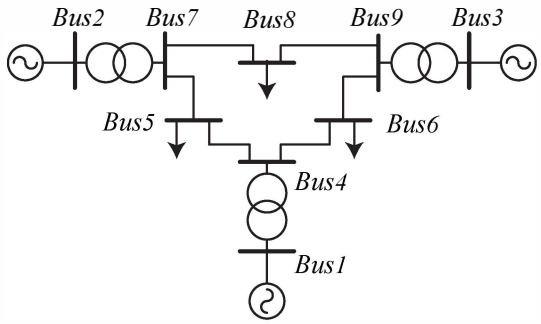

Fig. 6. 9-bus test system

A. Test for the SVC model

An SVC was installed at Bus 8, where a 16.67% load increase (both active power and reactive power) was applied at $t = 2$ s. Fig. 7 shows the SE computation results for multiple snapshots.

As shown in Fig. 7, the estimation residuals reach below 10^{-13} after relatively few iterations. This high accuracy results from the consistency between the network model used in the SE and the test system in PSAT. If the measurements for SE were acquired from an off-line simulation in another simulation tool or directly from PMUs, it is expected to

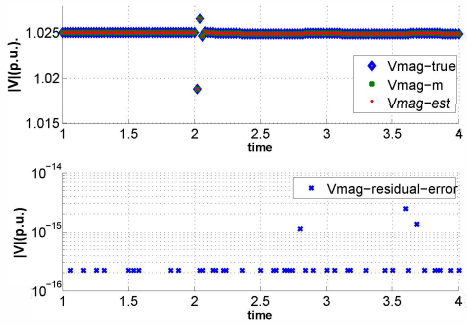

(a) Voltage magnitudes at Bus 8 for multiple snapshots

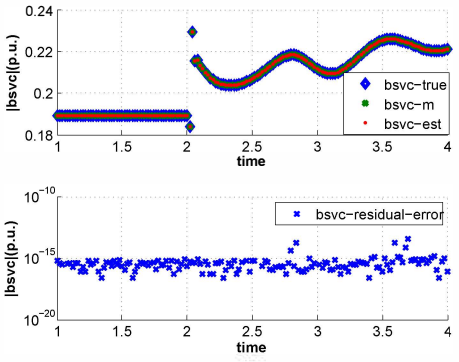

(b) b_{svc}

Fig. 7. SE of the 9-bus system with an SVC for multiple snapshots

obtain a lower accuracy as a result of uncertainties in the measurements and models.

Another issue that needs to be noticed is that for some snapshots the residuals are missing as they are smaller than the machine's precision. This also applies to the following test cases.

B. Test for the STATCOM model

The same scenario in Section V-A was also applied on the test system with an STATCOM installed at Bus 8. Fig. 8 shows the SE computation results for multiple snapshots. As it can be seen, the residuals before the perturbation occurred are below 10^{-13}, which is relatively close with the results in Section V-A. However, after the instance when the perturbation occurs, the estimation residuals increase to about 10^{-5}.

C. Test for the TCSC model

A TCSC was installed on the line between Bus 5 and Bus 4, and a fault was applied at Bus 3 from $t = 2$ s to $t = 2.04$ s. Figure 9 shows the SE computation results for multiple snapshots, where y_{tc} denotes the line admittance with considering the TCSC. The residuals increase immediately at the instance when the fault was applied, from around 10^{-13} to 10^{-3}.

D. Test for the SSSC model

The same scenario in V-C was applied on the test system with an SSSC installed on the line between Bus 5 and Bus 4. Figure 10 shows the SE computation results for multiple

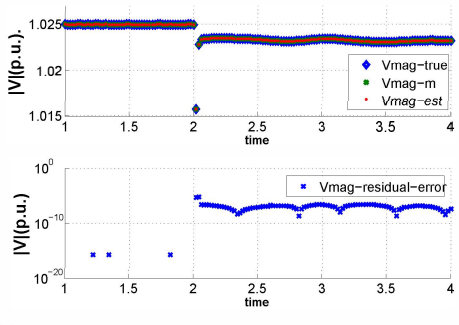

(a) Voltage magnitudes at Bus 8 for multiple snapshots

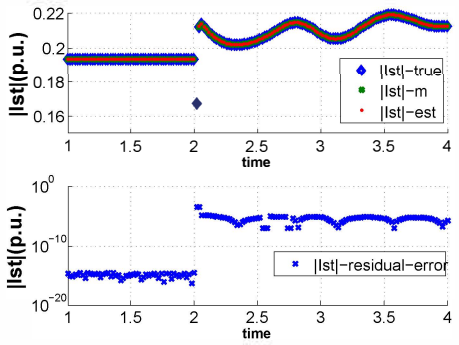

(b) I_{st}

Fig. 8. SE of the 9-bus system with an STATCOM for multiple snapshots

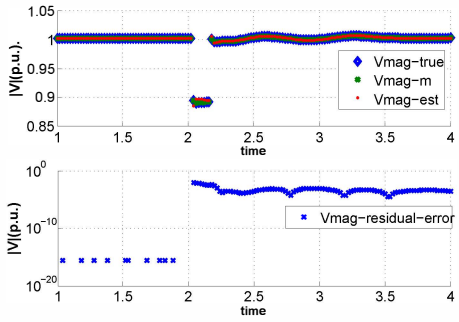

(a) Voltage magnitudes at Bus 5 for multiple snapshots

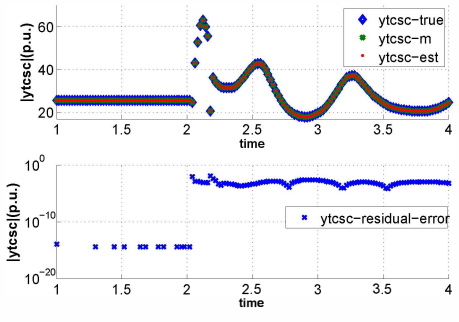

(b) y_{tc}

Fig. 9. SE of the 9-bus system with a TCSC for multiple snapshots

snapshots. The residuals increase immediately at the instance when the fault was applied, from around 10^{-13} to 10^{-3}.

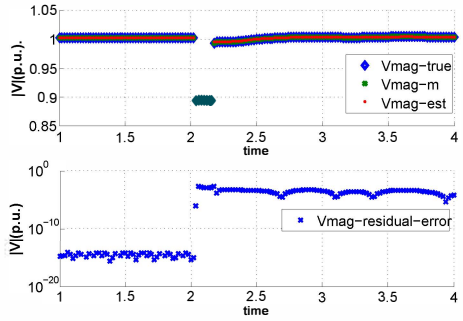

(a) Voltage magnitudes at Bus 5 for multiple snapshots

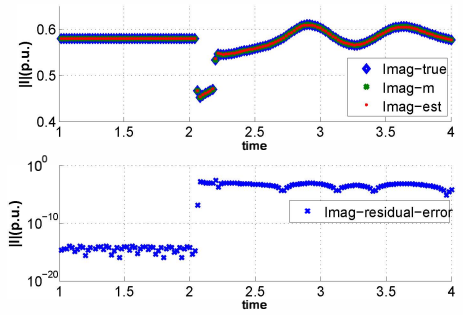

(b) Current magnitudes on the line between Bus 5 and Bus 4 for multiple snapshots

Fig. 10. SE of the 9-bus system with an SSSC for multiple snapshots

VI. Conclusions

A PMU-based state estimation algorithm that considers the presence of FACTS devices has been presented in this paper. Four common FACTS devices are modeled in a way that accommodates to the fast computation requirements of PMU-based SEs. In addition, the proposed algorithm separates measurement variables from the network model so that missing measurements will not affect the network model. This algorithm together with FACTS models is validated through study cases on a 9-bus system, which achieves a relatively accurate and fast SE performance.

Future work will focus on improving the estimation accuracy when the system is under large dynamic changes. Testing results indicate that additional modeling details may need to be included to obtain higher accuracy during large disturbances. However, for practical applications and operation within the linear response of the devices, the accuracy level is sufficient without increasing the computational burden.

References

[1] N. G. Hingorani, and L. Gyugyi, *Understanding FACTS–CONCEPTS AND TECHNOLOGY OF FLEXIBLE AC TRANSMISSION SYSTEMS*. New York: IEEE Press, 2000.

[2] A-A. Edris, *et al*, "Proposed Terms and Definations for Flexible AC Transmission System (FACTS)," *IEEE Trans. Power Delivery*, vol. 12, no. 4, pp. 1848-1853, Oct. 1997.

[3] A. Monticelli, *State Estimation in Electric Power Systems–A Generalized Approach*. Massachusetts: Kluwer Academic Publishers, 1999.

[4] W. Li, and L. Vanfretti, "Inclusion of Classic HVDC links in a PMU-Based State Estimator," *IEEE PES General Meeting*, July 2014.

[5] W. Li, and L. Vanfretti, "An Algorithm For Real-Time PMU-Based State Estimation Considering Classic HVDC Links Under Different Control Modes," *Sustainable Energy, Grids and Networks*, submitted, Sep. 2014.

[6] L. Vanfretti, J. H. Chow, S. Sarawgi, B. Fardanesh, "A Phasor-Data-Based State Estimator Incorporating Phase Bias Correction," *IEEE Trans. Power Syst.*, vol. 26, no. 1, pp. 111-119, Feb. 2011.

[7] S. G. Ghiocel, J. H. Chow, *et al.*, "Phasor-Measurement-Based State Estimation for Synchrophasor Data Quality Improvement and Power Transfer Interface Monitoring," *IEEE Trans. Power Syst.*, vol. 29, no. 2, pp. 881-888, March 2014.

[8] Phadke, A.G.; Thorp, J.S.; Karimi, K. J., "State Estimation with Phasor Measurements," *IEEE Trans. Power Syst.*, vol. 1, no. 1, pp. 233-238, Feb. 1986.

[9] F. Milano, *Power System Modeling and Scripting*. London, UK: Springer-Verlag, 2010.

[10] F. Milano, *Power System Analysis Toolbox Manual-Documentation for PSAT VERSION 2.1.6*, May 13, 2010.

[11] F. Milano, "An Open Source Power System Analysis Toolbox," *IEEE Trans. Power Syst.*, vol.20, no.3, pp.1199,1206, Aug. 2005.